Hindawi Publishing Corporation
Advances in Acoustics and Vibration
Volume 2009, Article ID 647658, 8 pages
doi:10.1155/2009/647658

Research Article

Evaluation of Defects in Multilayer Carbon Fibre Epoxy for Aeronautics Applications

M. Buonsanti,[1] M. Cacciola,[2] S. Calcagno,[2] G. Megali,[2] F. C. Morabito,[2] D. Pellicanò,[2] and M. Versaci[2]

[1] *MECMAT Department, Faculty of Engineering, University "Mediterranea" of Reggio Calabria, Via Graziella Feo di Vito, 89100 Reggio Calabria, Italy*
[2] *DIMET Department, Faculty of Engineering, University "Mediterranea" of Reggio Calabria, Via Graziella Feo di Vito, 89100 Reggio Calabria, Italy*

Correspondence should be addressed to M. Cacciola, matteo.cacciola@unirc.it

Received 23 February 2009; Accepted 3 June 2009

Recommended by Mohammad Tawfik

Production of carbon fibre reinforced polymers is an elaborate process unfree from faults and problems. Problems during the manufacturing, such as plies' overlapping, can cause flaws in the resulting material, so compromising its integrity. Compared with metallic materials, carbon epoxy composites show a number of advantages. Within this framework, ultrasonic tests are effective to identify the presence of defects. In this paper a Finite Element Method approach is proposed for evaluating the most effective incidence angle of an ultrasonic probe with regard to defects' identification. According to our goal, the analysis has been carried out considering a single-line plane emitting source varying the probe angle of inclination. The proposed model looks promising to specially emphasize the presence of delaminations as well as massive breaking in a specimen of multilayer carbon fibre epoxy. Subsequently, simulation parameters and results have been exploited and compared, respectively, for a preliminary experimental in-lab campaign of measurements with encouraging results.

1. Introduction

Within the framework of the aeronautic industry, the attention is focused on the quality check of the manufacture process, especially for the composite materials used in energy production (nuclear plants), transportation (aeronautic), workpiece manufacturing, and so forth. Composite materials, in particular Carbon Fibre Epoxy (CFRP/E), are also applied to various fields of aeronautic industry. Particularly, multi-layers CFRP/E are the basic product for constructing main parts of modern airplanes, which are subjected to a continuous degradation. Mechanic solicitations and atmospheric agents are responsible for a relatively rapid degradation of airplanes' structures. Therefore, they must be produced in an almost perfect state, in order to not introduce other dangerous risk factors. The manufacture process of CFRPs can induce a number of characteristic flaws, for example, delaminations, inclusions, and porosities. Therefore, it is absolutely necessary to carry out cheap tests of conformity and integrity. In particular Ultrasonic Testings (UTs) are useful for our aims, as it is possible to easily analyze even highly thick metallic as well as nonmetallic materials, with a good resolution and a remarkable operative versatility. The paper is structured as follows. Section 2 describes physical characteristics of CFRP/E materials. Section 3 is an overview of UTs technique. Section 4 presents the Finite Element Analysis (FEA) approach. Section 5 illustrates the results of the proposed approach to detect the kind of defect.

2. Physical Characteristics and Problems in CFRP/E

CFRPs are widely used in military and aerospace industries and in such applications in which high costs are justified by the increased performance of the final product (e.g., and racing cars, high-end automotive products, aerospace). Two major advantages are offered by CFRPs. First of all, high

mechanical properties are offered in terms of high stiffness-to-weight and resistance to weight ratios. The Ashby charts presented in Figure 1 show that fibre-reinforced materials in general, and particularly CFRP/E, have a combination of high mechanical properties in terms of stiffness, strength, and fracture toughness. If compared with engineering alloys, that have specific stiffness similar to CFRP/Es, higher specific strength and higher specific fracture toughness are offered. Moreover, if CFRP/Es are compared to engineering ceramics, a better fracture toughness is evident. Compared with common engineering materials, such as steels or cast irons, fibre-reinforced polymers present lower absolute values for Young modulus and tensile strength, but they offer much better specific properties (they have ten times smaller density). However, in terms of fracture toughness, the values are reasonably similar. The second main advantage offered by fibre-reinforced composites concerns the possibility to prepare customized materials in relation to final product requirements. In composite materials, the shape, the thickness, and the mechanical properties of the specimen can be controlled in order to satisfy specific requirements. Material form and fibre orientations can be chosen in relation to the design process and the material can be minutely controlled, minimizing weight and optimizing overall properties. If the stresses encountered by a load-bearing composite component in service are known, it is possible to design the fibre in order to optimize the stiffness-to-weight and strength-to-weight parameters of the component [1].

As pointed out in the introduction section, in recent years there is a growing interest in the use of low-cost heavy carbon fibre tows in textile composite applications, including Multi-Layers Fabrics (MLFs). The mechanical properties of these materials depend on the obtained crystallization. It depends on the peak value of the temperature and the speed during its manufacturing. Generally speaking, a brief final treatment at a temperature of 3000 °C increases significantly the fibres quality, increasing the value of Young modulus. It is possible to increase the strength and elastic modulus of these fibres through a hot-stretching. In this way, we obtain a poly-crystalline structure of carbon with the following excellent mechanical properties:

(i) tensile (R_m) = 1980 – 2570 N/mm^2

(ii) elastic module (E) = 220000 – 400000 N/mm^2

(iii) density (γ) = 1.75 Kg/dm^3.

The use of "nude" fibres does not allow to achieve structural parts subjected to a tension variable field. For this reason, the fibres are intimately linked (impregnated) with resins, which constitutes the previously introduced matrix.

The elementary structure of carbon fibres has a diameter range from 7 to 10 μm: typically the structure consists of filaments and about 3000 fibres compose a single filament. The carried out structure can be ordered with parallel filaments in order to form "unidirectional" specimen. Frequently, in aeronautic industry, preimpregnated fibres are usually purchased; its thickness goes from 0.1 to 0.3 mm. In order to have a good resistance with a tension variable field, the prefilled is layered with different orientation, forming a structure called "laminate". The thickness of the laminate goes from 10 to 20–25 mm.

The mechanical properties of a laminate structure are typically lower than "nude" fibres, and in particular:

(i) tensile (R_m) = 1270 – 1370 N/mm^2

(ii) elastic module (E) = 150000 – 200000 N/mm^2

(iii) density (γ) = 1.5 – 1.57 Kg/dm^3.

Composite materials are also subject to the presence of defects compromising the structural integrity of the same materials and, consequently, of aeronautic vehicles.

(i) *Delamination*. separation between two close layers along a horizontal plane; it is due to existing (air) or created (contamination) gas during the polymerization. Grouped little delaminations (resembling to flattened pores), distributed at different depths, are sometimes called microdelaminations.

(ii) *Inclusion* foreign material (e.g., the one used for the bag) accidentally left in the part during the lay-up.

(iii) *Porosity*. spherical/elliptical microvoid distributed within a volume or in parallel plane to a lay-up. Generally it is induced by incorrect pressure and temperature gradients during polymerization.

These factors may affect the performance of the composite material. However, the entity of the risk depends on the geometry of structure and on the effective localization and orientation of the defects. Similarly to metal structures, aeronautic composite structures are formed by several components assembled through pasting and screwing. This manufacturing techniques can produce the presence of defects, such as abscission between layers (due to pasting) or drilling (due to screwing). The presence of this kind of defects can cause the reduction of cohesion and adhesion resistance. Thus, the final properties of composite materials are intrinsically linked to the manufacturing process. In this framework, a good compromise between resistance, weight, and cost of aircraft structures is the main goal. In the next section the Ultrasound technique and the Finite Elements approach will be shown in order to inspect multi-layer plates, with oriented layer at 0°, 90°, 0° respectively, and reinforced with epoxy resin.

3. The Principle of the Ultrasound Method

When ultrasound method is used for imaging, one or two directional tones are transmitted via a transducer into the air. Subsequently, the reflections of the acoustic waves are recorded and exploited in order to determine various properties of the object under examination. Therefore, the propagation of directed single tone ultrasound is examined. This section presents a detailed background on acoustic propagation, focusing on the propagation of single tone plane waves. For this purpose, it is worthwhile to resume the fundamentals of particle oscillation governing the transmission of acoustic waves through a medium. This section gives a general overview of the physical equations that govern both

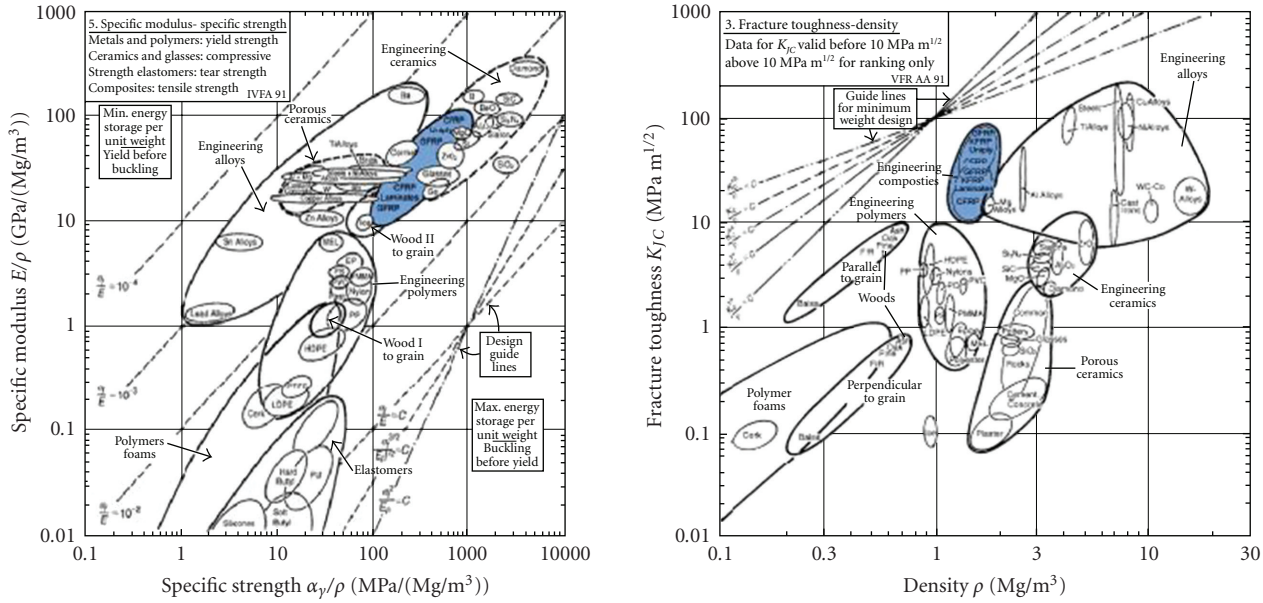

(a) Specific Young modulus is plotted versus specific strength.

(b) Fracture toughness is plotted versus density.

Figure 1: Ashby Material Property.

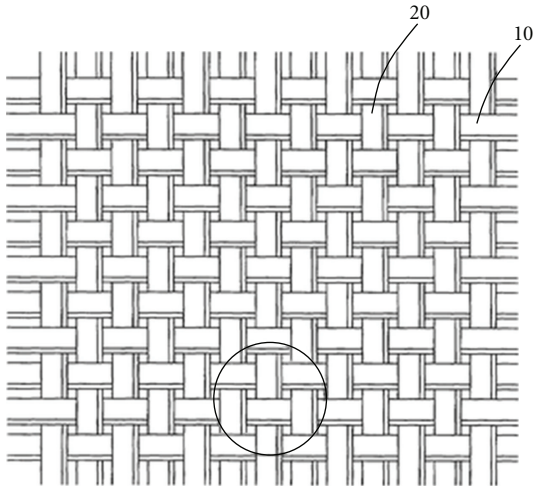

Figure 2: Example of the architecture of MLFs. Layers of unidirectional oriented fibres, made of adjacent spread tows, are stacked together automatically and then fixed with stitching.

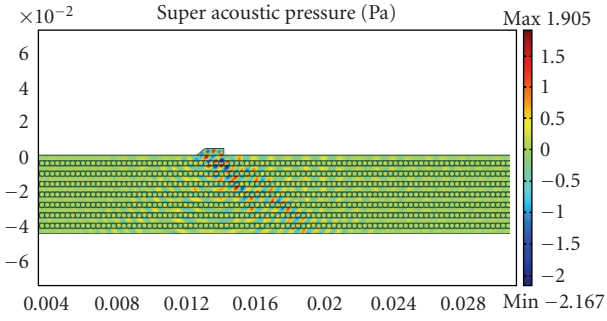

Figure 3: FEM-based implemented model.

linear and nonlinear wave motion through the air. It presents the partial differential equation that describes the pressure variation of a medium when a single frequency acoustic wave propagates.

Acoustic waves are pressure disturbances in the form of vibrational waves that propagate through a compressible medium. These vibrational waves displace the molecules of the medium from their quiescent point, after which a restoring elastic force pulls the molecules back. This elastic force, along with inertia, causes the oscillation of the molecules, allowing acoustic waves propagation.

The oscillatory motion is analogous to the motion of a spring when it is displaced from its rest position, while the propagation of the wave is analogous to the movement of a wave down a piece of string. The most well-known acoustic waves are those of sound. The audible frequency range for an average person is included from 20 Hz to 20 kHz; the range above the audible (greater than 20 kHz) is called the ultrasonic region. When we consider planar waves we mean that each acoustic variable has constant amplitude on any given plane perpendicular to the direction of propagation. This assumption greatly simplifies the derivations of acoustic equations and relationships. It is valid in most experimental situations because wave fronts of any divergent wave in a homogeneous medium become approximately planar, when sufficiently far from the source:

$$R = \frac{l^2}{\lambda}, \tag{1}$$

where l is the length of the source, λ is the wavelength of the wave and, R is the measuring distance from the source [2]. The acoustic waves are caused by pressure fluctuations in a compressible mean. In order to develop an equation for

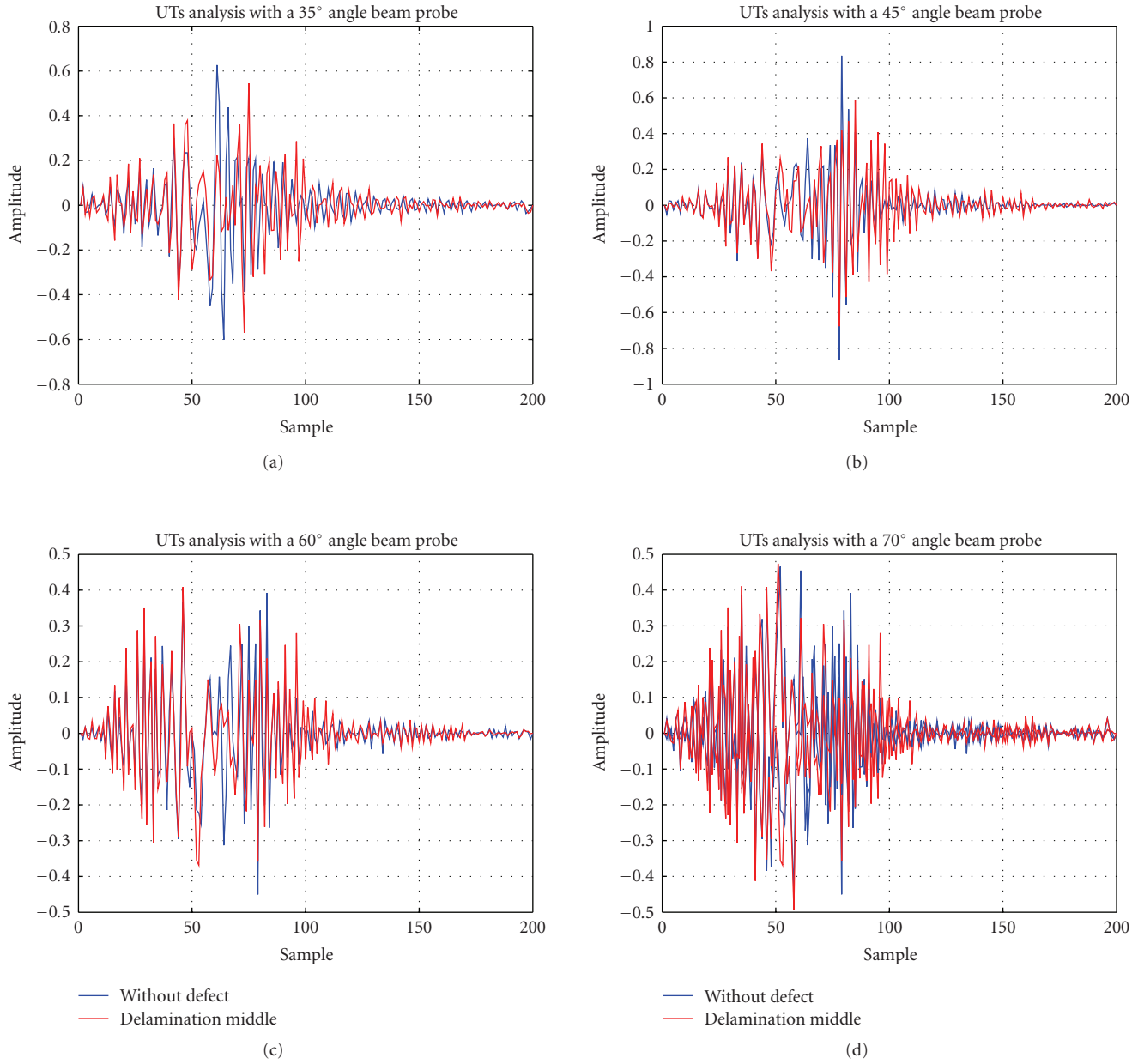

Figure 4: Ultrasound wave propagations results of FEA model.

acoustic wave propagation, it is possible to begin with the ideal case of propagation through a fluid. A nonviscose fluid is a particular fluid in which the effects of friction due to viscosity can be ignored, meaning that the viscous effects are relatively small compared with the inertial restoring forces of the fluid.

It also means that losses due to attenuation through the media can be ignored, making this a lossless equation for acoustic propagation. This equation is often a valid approximation, because, frequently, dissipation is so small that it can be ignored for the frequencies or distances of interest. Using the governing physical equations for sound, the linear wave equation can be derived [3]. These equations are the linear equation of state (2), the linear equation of continuity (3), and the linear equation of force (4), also known as Euler's Equation:

$$p \approx B^* s_c, \tag{2}$$

$$\frac{\partial \rho}{\partial t} + \rho_0 \nabla \vec{u} = 0, \tag{3}$$

$$\rho 0 \frac{\partial \vec{u}}{\partial t} = -\nabla p. \tag{4}$$

Combining (2), (3), and (4), it is possible to consider a single differential equation with one dependant variable

$$\nabla^2 p - \frac{1}{c^2} \frac{\partial^2 p}{\partial t^2} = 0. \tag{5}$$

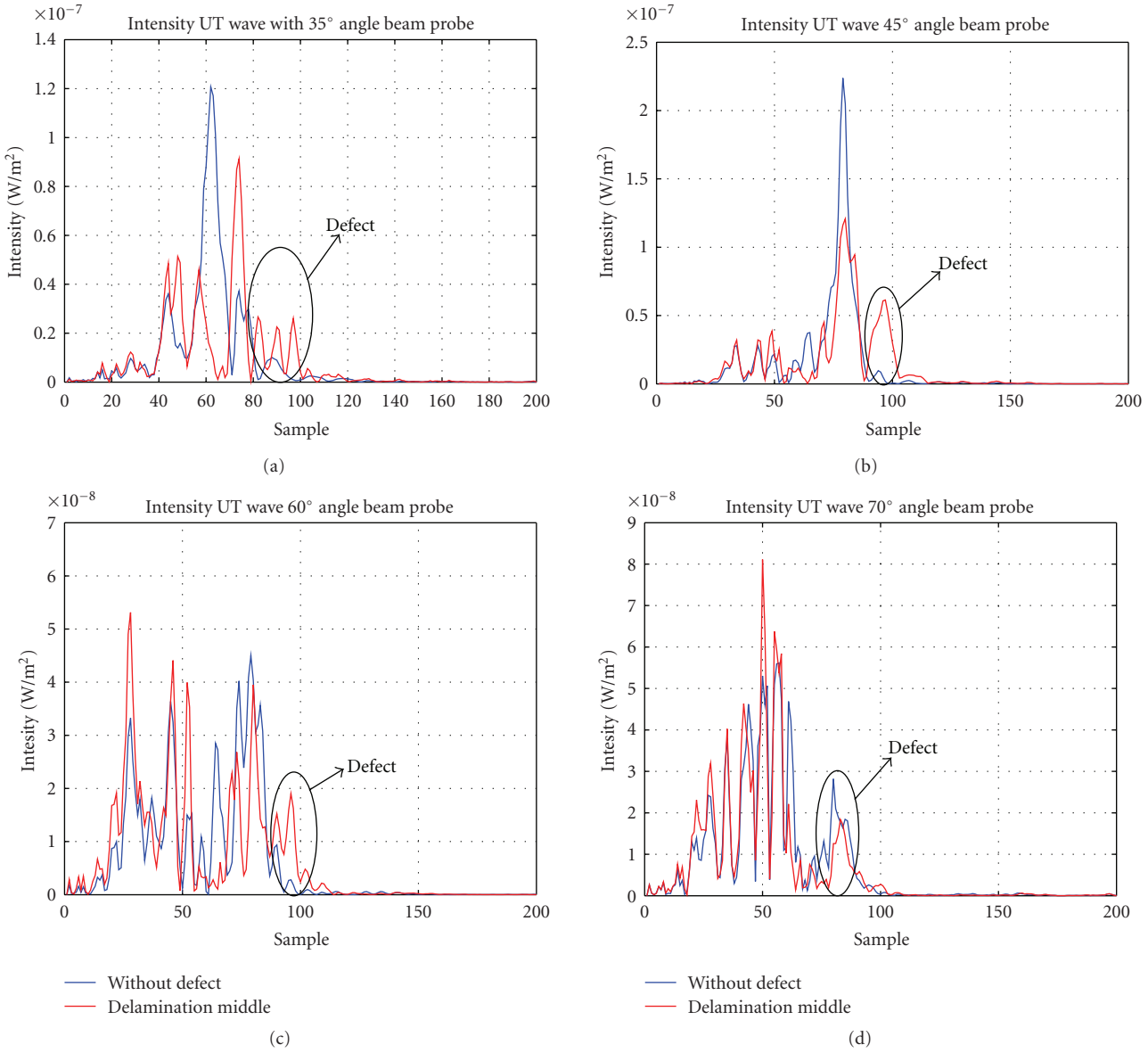

Figure 5: Intensity of the UT wave.

This equation is the linear, lossless wave equation for the propagation of sound in fluids with phase speed c_0. The equation for one-dimensional wave propagation, whose solutions is known, can be written as follows:

$$p(x,t) = P_0 \cos(\omega_0 t - kx). \tag{6}$$

Including the viscosity, the ideal hypothesis is not valid and the Euler's equation must be changed with the inclusion of viscosity effects term to the right side:

$$\rho \frac{\partial \vec{u}}{\partial t} + \nabla p = \left(\frac{3}{4}\eta + \eta_B\right) \nabla(\nabla \cdot \vec{u}) - \frac{1}{2}\rho_0 \nabla^2 \vec{u}, \tag{7}$$

where η is the shear viscosity coefficient and η_B is the coefficient of bulk viscosity. Combining (2), (3), and (7) is possible to obtain a single differential equation with one dependant variable:

$$\nabla^2 p - \frac{1}{c^2}\frac{\partial^2 p}{\partial t^2} + \frac{0.75\eta + \eta_B}{\rho_0 {c_0}^2} \nabla^2 \frac{\partial p}{\partial t} = 0. \tag{8}$$

This equation is the linear, dissipative wave equation for the propagation of sound in fluids.

Note that it is identical to the lossless equation except for the added third term on the left hand side, that is, the viscous dissipative term.

For a plane wave travelling in the positive x direction, the solution of (8) is defined as follows:

$$p(x,t) = P_0 e^{(-\alpha x)} \cos(\omega_0 t - kx), \tag{9}$$

where α is the attenuation coefficient in Np/m which causes the amplitude to decay in an exponential form. Plane waves

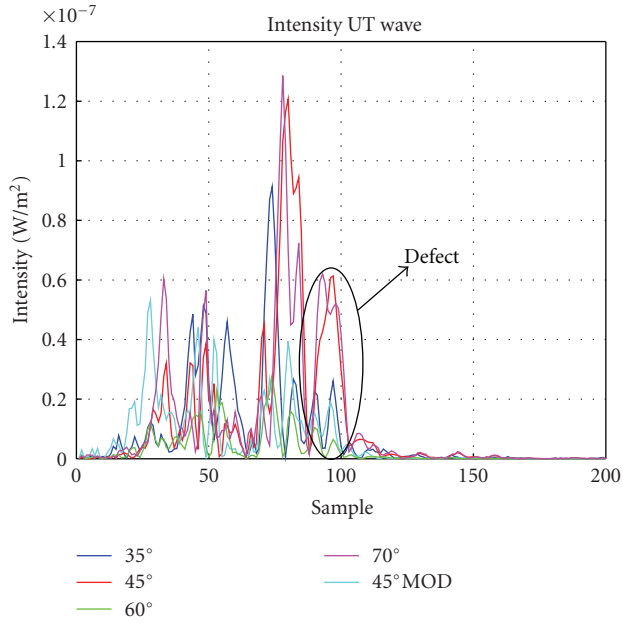

Figure 6: Comparison of UT waves' intensities.

are a special case in the study of acoustic propagation because they propagate in a single direction and they also have constant amplitude and phase on any plane perpendicular to the direction of propagation. Generally, the majority of waves can be considered as planar when sufficiently far from the source point. The solution for the pressure field $p(x,t)$ of a plane wave is described by (6). So, the velocity and velocity potential equations of a plane wave can easily be derived. Due to inherent properties of the plane wave, above described, the velocity of the wave differs from pressure by a constant:

$$\vec{u}(x,t) = \frac{\vec{p}(x,t)}{\rho_0 c_0}, \tag{10}$$

where $\rho_0 c_0$ is defined for a specific acoustic impedance Z_0 of the media. This impedance is analogous to the wave impedance $\sqrt{\mu/\varepsilon}$ of a dielectric medium for electromagnetic waves, or to the characteristic impedance of a transmission line. The velocity potential equation is similarly obtained and it is related to pressure by a complex constant

$$\vec{\Psi}(x,t) = \frac{\vec{p}(x,t)}{j\omega_0\rho_0}. \tag{11}$$

The linear relationship between pressure and velocity is very useful, especially with the development of equations for acoustic intensity.

The instantaneous intensity in W/m^2 of an acoustic wave is

$$I(t) = \vec{p}(x,t) * \vec{u}(x,t). \tag{12}$$

Theoretical approach described in this section has been exploited for the simulation step in order to obtain software measurements. FEA-based approach and data collection will be described in the next section.

Table 1: Geometrical parameters of the model.

Parameter	Dimension
Plate dimension	50 mm × 5 mm
Fibre diameter	0.3 mm
Number of layers	15

4. FEA Approach

In this section we show the proposed model. We propose an Ultrasound FEA model in order to evaluate the presence of delaminations in multi-layer plates of carbon fibre reinforced. They are characterized by different layers, oriented at 0°, 90°, 0° respectively, and reinforced with epoxy resin [4]. The UTs technique is analysed by a numerical model. Finite Element Method- (FEM) based approach can supply an important support for a preliminary in-lab campaign of measurements. The model requires the geometrical and physical definition of the UTs probe and the CFRP/E specimen. The geometry of the system is presented in Figure 2; Table 1 resumes geometrical settings.

The proposed approach, based on UT inspection, exploits the acoustic pressure p [5–7] and has been carried out by a commercial code (Comsol Multiphysics).

In this way we calculated the acoustic pressure p in a general subdomain Ω:

$$\nabla\left(-\left(\frac{1}{\rho_c}\right)(\nabla p - q)\right) + \left(\frac{{k_z}^2}{\rho_c} - \frac{\omega^2}{(\rho_c {c_c}^2)}\right)p = Q, \tag{13}$$

where $\rho_c = k_c Z_c/\omega$ represents the complex fluid density; $c_c = \omega/k_c$ represents the complex speed of sound; $k_c = \omega/c_s - ia$ represents the complex wave number; $Z_c = \rho_0 c_s$ is the complex impedance; ρ_0 is the material density; c_s is the speed of the sound; a is the attenuation coefficient; ω is the angular pulsation; p represents the pressure; Q is the dipole source. For simulating the ultrasound wave, cylindrical wave formulation has been exploited in boundaries setting [8, 9]:

$$\begin{aligned}\mathbf{n}\cdot\frac{1}{\rho_0(\nabla p - q)} &= \left(ik + \frac{1}{2r} - \frac{1}{(8r(1+ikr))}\right)\frac{\left(p_0 e^{-i\mathbf{kr}} - p\right)}{\rho_0} \\ &\quad + \frac{r}{(2\rho_0(1+ikr))}\Delta_T\left(p - p_0 e^{-i\mathbf{kr}}\right) - \frac{i(\mathbf{k}\cdot\mathbf{n})p_0 e^{-j\mathrm{kr}}}{\rho_0},\end{aligned} \tag{14}$$

where p_0 is the source pressure.

All boundaries are modelled with the following conditions: absorbing and reflecting boundary conditions. Reflecting boundary conditions are modelled as Neumann conditions. Absorbing boundary conditions are also modelled as Neumann but with a weak constrain on the time term. In detail, boundaries conditions are set as follows.

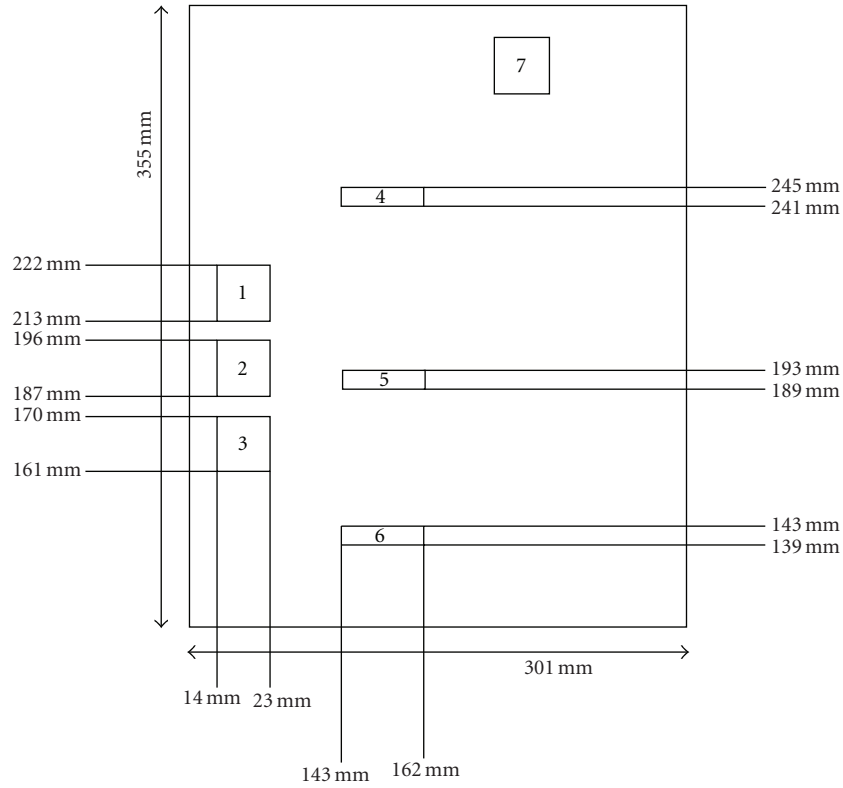

Figure 7: Specimen used for UTs measures.

Continuity Conditions. set to internal boundary of subdomain that represents the UTs wave interaction with the internal structure of examined material:

$$\mathbf{n}\cdot\left(\left(-\left(\frac{1}{\rho_0}\right)(\nabla p - q)\right)_1 - \left(-\left(\frac{1}{\rho_0}\right)(\nabla p - q)\right)_2\right) = 0. \tag{15}$$

Soft-Boundary Conditions. All boundary perimeter they are set up with this condition since the plate has a finite dimension:

$$p = 0. \tag{16}$$

Matched Boundary Conditions. Set to bottom boundary that represents the interaction of the UTs wave with the bottom of examined plate:

$$\mathbf{n}\cdot\left(\frac{1}{\rho_0(\nabla p - q)}\right) = \frac{\left(i(\omega^2/c^2 + k_1k_2)\left(p_0e^{-j\mathbf{kr}} - p\right) + \left(\Delta_T p_0 e^{-j\mathbf{kr}} - \Delta_T p\right)\right)}{(\rho_0(k_1 + k_2)) - i/\rho_0\mathbf{k}\cdot\mathbf{n}p_0e^{-j\mathbf{k}\cdot\mathbf{r}}}. \tag{17}$$

Table 2: Physical subdomain settings.

Parameter	Dimension
Speed Sound/Density [0°] fibres orientation	2000 m/s / 2.1 Kg/m^3
Speed Sound/Density [90°] fibres orientation	1360 m/s / 1.7 Kg/m^3
Speed Sound/Density Epoxy Resin	3000 m/s / 1.2 Kg/m^3
Attenuation Coefficient Carbon Fibre	4.3 e^{-6}
Attenuation Coefficient Epoxy Resin	50

The line source is modelled with a length equal to 0.6 mm. The final results of simulations are shown in Figures 3, 4, 5 and 6.

5. Simulations Results and In-Lab Measures

According our FEM approach, we obtained the useful information, resumed by Table 4, in order to detect the presence of defect during in-lab experimentations.

Table 3: Geometrical parameters of the probe.

Parameter	Dimension			
Height	20 mm			
Length	30 mm			
Source diameter	0.6 mm			
Angle	35°	45°	60°	70°

Table 4: Parameters of built probe.

Parameter	Dimension
Probe height	20 mm
Probe length	30 mm
Source diameter	0.6 mm
Best angle for defects detection	45°

They have been carried out on a specimen of $301 \times 355 \times 4$ mm panel containing delamination-like and no defect area (see Figure 7) in order to validate the results of our FEM approach, with the proposed UTs probe. On the basis of simulations arrangements, the measurements have been carried out with a fixed frequency value (5 MHz). During the scanning along x-axis the maximum of the UTs signal is placed under the probe, and decreasing away from the source [10]. Experimentations confirm the FEA simulations.

6. Conclusions

In this paper, a Finite Element Method (FEM) approach has been proposed. Single-line plane waves emitting sources have been modelled in order to investigate the most effective incidence angle with regard to defects' identification.

According to the FEM approach performances, it is possible to detect the presence of a delamination in the analysed structure. The exploited UT-based experimental methodology has satisfactory confirmed the model increases the ability of detecting very small delaminations in CFRP/Epoxy. This ability has been confirmed from the results obtained by experimental analysis. The UTs signal propagates inside the specimen. The interaction of the wave with the defect causes a reflection of the signal that generated the defect peak. Varying the angle of the probe, there is a different kind of detection of the flaw, as shown in Figure 6. From the numerical results, it is possible to note that the best resolution of defect detection is obtained by a probe inclination equal to 45 degree. Our FEA approach has been subsequently and successfully validated with in-lab measurements.

In conclusion, a future work would be predicting signal affected by noise for the probe used during simulations, that is, reduce the presence of echoes. Authors are actually engaged in this direction.

Nomenclature

$a(x,t)$: Particle acceleration
A: Oscillation amplitude
b: Nonlinear restoring force
c: Speed of wave propagation
c_s : Speed of sound propagation
f_0 : Source frequency
I : Intensity
I_{ref}: Reference intensity
K : Wave number
l : Length of source
m : Mass
p': Perturbation pressure
p_o: Equilibrium pressure
P_o: Initial pressure amplitude
$p(x,t)$: Acoustic pressure
R_m: Mechanical resistance
t: Time
u_o: Initial velocity
$u(x,t)$: Particle velocity

Acknowledgment

Many thanks to the scientists and technicians of Alenia Aeronautica SpA, Pomigliano d'Arco, Naples, Italy, for technical support and data disposal useful to write this paper. Property of collected data belongs to Alenia Aeronatica SpA, Turin, Italy.

References

[1] M. F. Ashby, *Material Selection in Mechanical Design*, Butterworth Heinemann, Oxford, UK, 2nd edition, 1999.
[2] B. A. Auld, *Acoustic Fields and Waves in Solids*, vol. 1, Krieger Publishing, Malabar, Fla, USA, 1990.
[3] A. Chakraborty and S. Gopalakrishnan, "A spectral finite element model for wave propagation analysis in laminated composite plate," *Journal of Vibration and Acoustics*, vol. 128, no. 4, pp. 477–488, 2006.
[4] A. A. Baker and B. C. Hoskin, *Composite Materials for Aircraft Structures*, AIAA Education Series, AIAA, 1986.
[5] D. T. Blackstock, *Fundamentals of Physical Acoustics*, Wiley, New York, NY, USA, 2000.
[6] O. C. Zienkiewicz, *The Finite Element Method*, McGraw-Hill, New York, NY, USA, 1989.
[7] R. B. Thompson and H. N. G. Wadley, "The use of elastic wave-material structure interaction theories in NDE modeling," *Critical Reviews in Solid State and Materials Sciences*, vol. 16, no. 1, pp. 37–89, 1989.
[8] J. M. Whitney, *Structural Analysis of Laminated Anisotropic Plates*, Technomic, Lancaster, Pa, USA, 1987.
[9] F. L. Matthews and R. D. Rawlings, *Composite Materials: Engineering and Science*, Chapman & Hall, Boca Raton, Fla, USA, 1996.
[10] M. Buonsanti, M. Cacciola, S. Calcagno, F. C. Morabito, and M. Versaci, "Ultrasonic pulse-echoes and eddy current testing for detection, recognition and characterisation of flaws detected in metallic plates," in *Proceedings of the 9th European Conference on Non-Destructive Testing*, Berlin, Germany, 2006.